

# Modeling metallic fatigue data using the Birnbaum–Saunders distribution

Zaid Sawlan<sup>a,\*</sup>, Marco Scavino<sup>b</sup>, Raúl Tempone<sup>c,d</sup>

<sup>a</sup>*Department of Mathematics, King Fahd University of Petroleum and Minerals, Dhahran, Saudi Arabia*

<sup>b</sup>*Instituto de Estadística (IESTA), Universidad de la Repùblica, Montevideo, Uruguay*

<sup>c</sup>*CEMSE, King Abdullah University of Science and Technology, Thuwal, Saudi Arabia*

<sup>d</sup>*Chair of Mathematics for Uncertainty Quantification, RWTH Aachen University, Aachen, Germany*

---

## Abstract

This work employs the Birnbaum–Saunders distribution to model metallic fatigue and compares its performance to fatigue-limit models based on the normal distribution. First, we fit data for 85 fatigue experiments with constant amplitude cyclic loading applied to unnotched sheet specimens of 75S-T6 aluminum alloys. The fit obtained by the Birnbaum–Saunders distribution is noticeably better than the normal distribution. Then, we define new equivalent stress for two fatigue experiment types: tension-compression and tension-tension. With the new equivalent stress, the statistical fit improves for both distributions, with a slight preference for the Birnbaum–Saunders distribution. In addition, we analyze a dataset of rotating-bending fatigue experiments applied to 101 round bar specimens of 75S-T6 aluminum. Finally, we consider a well-known dataset of bending tests applied to 125 specimens of carbon laminate. Overall, the Birnbaum–Saunders distribution provides better fit results under fatigue-limit models with various experimental setups.

**Keywords:** Metallic fatigue data; fatigue-life prediction; fatigue-limit models; maximum likelihood methods; Birnbaum–Saunders distribution

---

## 1. Introduction

Fatigue-life prediction is vital to preventing the failure of mechanical parts under cyclic loading. Stress-life models, or S-N curves, are usually used to model fatigue life [1, 2, 3]. Although many models relate stress to the fatigue life, with probabilistic models, the fatigue life is often assumed to be a log-normal random variable [4, 5, 6, 7] or to follow the Weibull distribution [4, 8]. This work considers Birnbaum–Saunders distributions and compares the fit of different fatigue datasets with the log-normal distribution.

Birnbaum–Saunders distributions were introduced as a two-parameter family of life distributions [9]. Several studies have used these distributions to fit fatigue datasets using the maximum likelihood (ML) [10, 11] and Bayesian methods [12, 13, 14]. In addition, many variations have been proposed, such as the log-linear model for the Birnbaum–Saunders distribution [15] and bivariate log Birnbaum–Saunders distribution [16]. An extensive review of the Birnbaum–Saunders distribution and its generalizations is provided in [17, 18].

We aim to study the use of Birnbaum–Saunders distributions and analyze their fit results compared with the dominant choice of normal distributions. Thus, we use two datasets of fatigue experiments applied to specimens of 75S-T6 aluminum alloys [19, 20] and a dataset of bending tests of carbon laminate [21].

---

\*Corresponding author

Email addresses: [zaid.sawlan@kfupm.edu.sa](mailto:zaid.sawlan@kfupm.edu.sa) (Zaid Sawlan), [marco.scavino@fcea.edu.uy](mailto:marco.scavino@fcea.edu.uy) (Marco Scavino), [raul.tempone@kaust.edu.sa](mailto:raul.tempone@kaust.edu.sa) (Raúl Tempone)

For the S-N models, many possible regression models could be considered. We focus only on the fatigue-limit models with constant and nonconstant variance (or the shape parameter). The fatigue-life variable is modeled by the log-normal distribution or Birnbaum–Saunders distribution. Equivalently, the logarithm of  $N$  is modeled by the normal and sinh-normal distributions, respectively. However, we demonstrate that modeling  $\log(N)$  as a Birnbaum–Saunders distribution improves the fit results. This proposed model is unprecedented in the literature, to the best of our knowledge.

The first dataset is the same data considered in [4], where fatigue-limit models and random fatigue-limit models were calibrated using the normal and Weibull distributions. We recalibrate fatigue-limit models using the Birnbaum–Saunders distribution. In addition, we propose a new equivalent stress model that accommodates different experiment types in Dataset 1. For Dataset 2, fatigue data corresponds to rotating-bending experiments applied to round bar specimens with different minimum-section diameters. Again, we calibrate fatigue-limit models and compare the fit of the normal and Birnbaum–Saunders distributions. As Dataset 3, we use the laminate panel data [21, 5], and calibrate and compare our proposed models.

This paper is organized as follows. Section 2 considers the fatigue data for unnotched sheet specimens of 75S-T6 aluminum alloys. Six variations of fatigue-limit models are introduced in Section 2, comparing stress-life models fitted to the data using the normal and Birnbaum–Saunders distributions. Next, Section 3 proposes a new equivalent stress definition to eliminate the effect of the experiment type. Then, Section 4 presents fatigue data corresponding to the unnotched round bar specimens of different sizes, followed by calibration and model comparison. Then, laminate panel data are fitted and analyzed in Section 5 using the predefined fatigue-limit models. Finally, the conclusions are presented in Section 6.

## 2. Model calibration and comparison for Dataset 1

### 2.1. Description of Dataset 1

Dataset 1 consists of 85 fatigue experiments that applied constant amplitude cyclic loading to unnotched sheet specimens of 75S-T6 aluminum alloys [19, Table 3, pp. 22–24]. The following data are recorded for each specimen:

- maximum stress,  $S_{max}$ , measured in ksi units;
- cycle ratio,  $R$ , defined as the minimum to maximum stress ratio. The ratio  $R$  is positive when the experiment corresponds to tension-tension loading and negative when the experiment corresponds to tension-compression loading;
- fatigue life,  $N$ , defined as the number of load cycles at which fatigue failure occurred; and
- a binary variable (0/1) to denote whether the test stopped before failure (run-out).

In 12 of the 85 experiments, the specimens remained unbroken when the tests were stopped.

### 2.2. Fatigue-limit models

The fatigue life should be modeled for a stress quantity defined for any cycle ratio. Therefore, we use Walker's model to define the equivalent stress:

$$S_{eq} = S_{max}(1 - R)^q, \quad (1)$$

where  $q$  is a fitting parameter. In the upcoming sections, we consider fatigue-limit models where the location parameter is given by  $A_1 + A_2 \log_{10}(S_{eq} - A_3)$  and the fatigue-limit parameter  $A_3$  is a threshold parameter where fatigue life becomes infinite when the equivalent stress is lower than  $A_3$ . Multiple fatigue-limit models could be created based on the choice of the distribution of the fatigue life,  $N$ . We consider three choices as follows.

### 2.2.1. Model Ia

In Model Ia, we assume fatigue life is modeled using a log-normal distribution, or equivalently, that  $\log_{10}(N)$  is modeled with a normal distribution with a mean of

$$\mu(S_{eq}) = A_1 + A_2 \log_{10}(S_{eq} - A_3), \text{ if } S_{eq} > A_3 \quad (2)$$

and a constant standard deviation of  $\sigma(S_{eq}) = \tau$ . Moreover, fatigue experiments are assumed independent, and run-outs are modeled using the survival probability. Thus, the likelihood function for Model Ia is given by

$$L(A_1, A_2, A_3, \tau, q; \mathbf{n}) = \prod_{i=1}^m \left[ \frac{1}{n_i \log(10)} g(\log_{10}(n_i); \mu(S_{eq}), \tau) \right]^{\delta_i} \left[ 1 - \Phi \left( \frac{\log_{10}(n_i) - \mu(S_{eq})}{\tau} \right) \right]^{1-\delta_i},$$

where  $g(t; \mu, \sigma) = \frac{1}{\sqrt{2\pi}\sigma} \exp \left\{ -\frac{(t-\mu)^2}{2\sigma^2} \right\}$ ,  $\Phi$  is the cumulative distribution function of the standard normal distribution, and

$$\delta_i = \begin{cases} 1 & \text{if } n_i \text{ is a failure} \\ 0 & \text{if } n_i \text{ is a run-out.} \end{cases}$$

### 2.2.2. Model IIa

For Model IIa, we assume fatigue life is modeled using the Birnbaum–Saunders distribution, or equivalently, that  $\log(N)$  is modeled with a sinh-normal distribution [18] with a constant shape parameter  $\alpha$ , a scale parameter of 2, and a location parameter  $\mu(S_{eq})$  given by (2). Under this assumption, the likelihood function for Model IIa is given by

$$L(A_1, A_2, A_3, \alpha, q; \mathbf{n}) = \prod_{i=1}^m \left[ \frac{1}{n_i} g(\log(n_i); \alpha, \mu(S_{eq})) \right]^{\delta_i} \left[ 1 - \Phi \left( \frac{2}{\alpha} \sinh \left( \frac{\log(n_i) - \mu(S_{eq})}{2} \right) \right) \right]^{1-\delta_i},$$

where  $g(y; \alpha, \mu) = \frac{1}{\alpha \sqrt{2\pi}} \cosh \left( \frac{y-\mu}{2} \right) \exp \left( -\frac{2}{\alpha^2} \sinh^2 \left( \frac{y-\mu}{2} \right) \right), y > 0$ , and  $\alpha, \mu > 0$ .

### 2.2.3. Model IIIa

For Model IIIa, we assume  $\log_{10}(N)$  is modeled using a Birnbaum–Saunders distribution with a constant shape parameter  $\alpha$  and a location parameter  $\mu(S_{eq})$ , given by (2). The resulting distribution for  $N$  is not the so-called log Birnbaum–Saunders distribution reported in [18]. However, the distribution of  $N$  is obtained similarly to deriving the log-normal distribution.

$$L(A_1, A_2, A_3, \alpha, q; \mathbf{n}) = \prod_{i=1}^m \left[ \frac{1}{n_i \log(10)} g(\log_{10}(n_i); \alpha, \mu(S_{eq})) \right]^{\delta_i} \left[ 1 - \Phi \left( \frac{1}{\alpha} \left( \sqrt{\frac{\log_{10}(n_i)}{\mu(S_{eq})}} - \sqrt{\frac{\mu(S_{eq})}{\log_{10}(n_i)}} \right) \right) \right]^{1-\delta_i},$$

where  $g(y; \alpha, \mu) = \frac{1}{\sqrt{2\pi}} \frac{(y+\mu)}{2\alpha\sqrt{\mu}y^{3/2}} \exp \left\{ -\frac{1}{2\alpha^2} \left( \frac{y}{\mu} + \frac{\mu}{y} - 2 \right) \right\}, y > 0$ , and  $\alpha, \mu > 0$ .

The three models are now fitted to Dataset 1 by maximizing the mentioned likelihood functions. Numerically, only the log-likelihood can be evaluated, and we maximize the log-likelihood instead. The ML estimates (MLEs) and the maximum log-likelihood value are reported in Table 1. The estimated parameters for Model IIa have a different scale compared with those in Models Ia and IIIa. The change in scale is only because Model IIa models  $\log(N)$  instead of  $\log_{10}(N)$ . However, all applied likelihood functions are normalized; therefore, the performance of the fit is not affected by the logarithm base selection.

The results in Table 1 indicate that Models Ia and IIIa provide the best fit for Dataset 1. We visualize the fit using the 0.05 and 0.95 quantile functions and the median function. The data can also be plotted

Table 1: Maximum likelihood estimates for Models Ia, IIa, and IIIa

	$A_1$	$A_2$	$A_3$	$q$	$\tau/\alpha$	Max $\log(L)$
Model Ia	7.38	-2.01	35.04	0.5628	0.5274	950.16
Model IIa	18.81	-5.68	33.11	0.5390	1.54	960.68
Model IIIa	7.22	-1.90	35.32	0.5574	0.0933	938.90

given the MLE of  $q$ . We distinguish data based on the experiment type or stress ratio. Figures 1 and 2 illustrate the quantile functions of Models Ia and IIIa obtained using the MLE parameters. The quantile functions of Model IIIa produce a better fit than those of Model Ia, which coincides with the fact that Model IIIa has the highest log-likelihood value among the three models in Table 1. We also observe that data seem segregated by the median according to the experiment type: tension-tension ( $R > 0$ ) and tension-compression ( $R < 0$ ). We analyze this behavior further in Section 3.

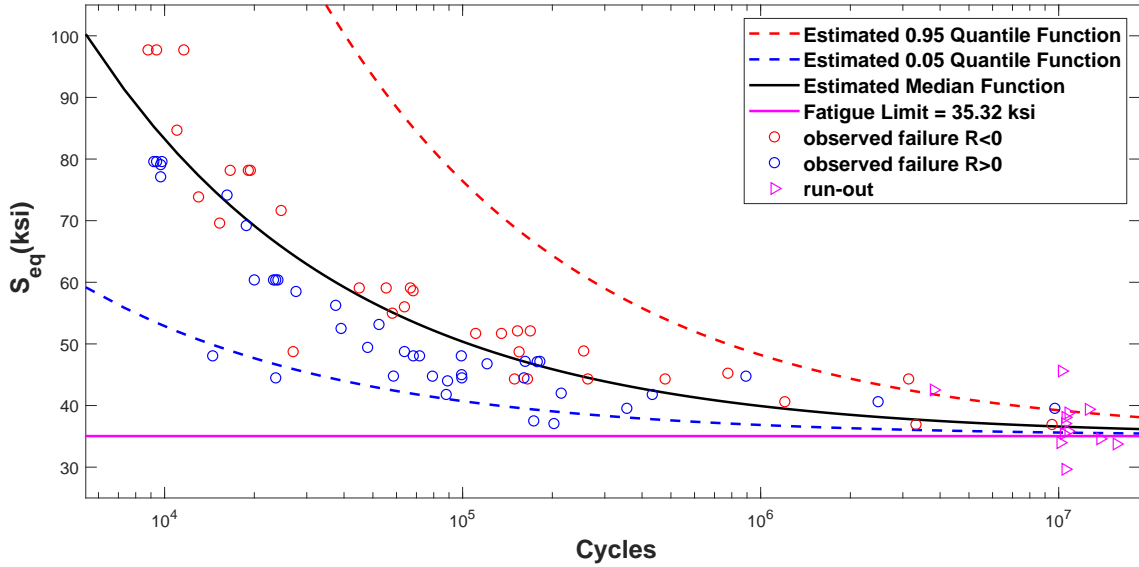


Figure 1: Model Ia:  $\log_{10}(N) \sim N(\mu(S_{eq}), \sigma)$  and  $S_{eq} = S_{max}(1 - R)^q$ .

We allow the standard deviation or shape parameter to be nonconstant to improve the fit of the three previous models. In particular, we assume this parameter is a function of the equivalent stress. With the same probability distributions previously considered, we introduce three new fatigue-limit models with nonconstant standard deviation/shape parameters.

#### 2.2.4. Model Ib

Analogous to Model Ia, for Model Ib, we assume  $\log_{10}(N)$  has a normal distribution with the mean function  $\mu(S_{eq})$  defined in 2. However, the standard deviation is assumed nonconstant and given by  $\sigma(S_{eq}) = 10^{(B_1 + B_2 \log_{10}(S_{eq}))}$ . The resulting likelihood function is equivalent to that derived for Model Ia.

#### 2.2.5. Model IIb

For Model IIb, the fatigue life  $N$  is modeled by the Birnbaum–Saunders distribution with location parameter  $\mu(S_{eq})$  (defined in 2) and nonconstant shape parameter  $\alpha(S_{eq}) = 10^{(B_1 + B_2 \log_{10}(S_{eq}))}$ .

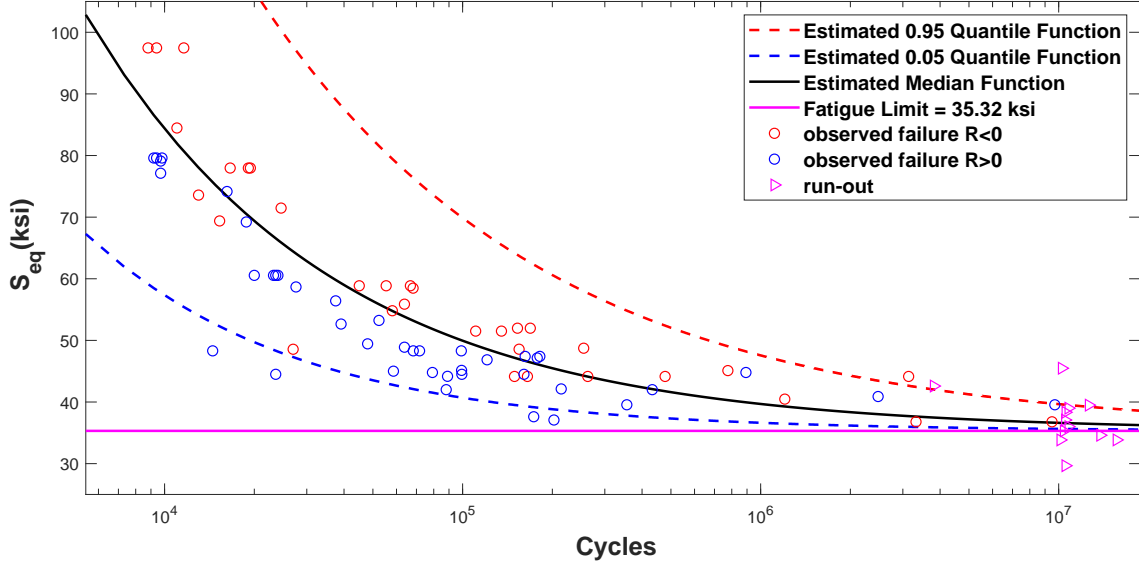


Figure 2: Model IIIa:  $\log_{10}(N) \sim BS(\alpha, \mu(S_{eq}))$  and  $S_{eq} = S_{max}(1 - R)^q$ .

### 2.2.6. Model IIIb

For Model IIIb,  $\log_{10}(N)$  is modeled using the Birnbaum–Saunders distribution with the location parameter  $\mu(S_{eq})$  and nonconstant shape parameter  $\alpha(S_{eq}) = 10^{(B_1 + B_2 \log_{10}(S_{eq}))}$ .

The new Models Ib, IIb, and IIIb are calibrated to fit Dataset 1, and the MLEs of the parameters of these models are presented in Table 2. Comparing the maximum log-likelihood values in Tables 1 and 2 reveals that the fit improved considerably for all models. In contrast, the difference between the new models decreased, with Model IIIb still providing the best fit.

Table 2: Maximum likelihood estimates for Models Ib, IIb, and IIIb

	$A_1$	$A_2$	$A_3$	$q$	$B_1$	$B_2$	Max log(L)
Model Ib	6.72	-1.57	36.21	0.5510	4.55	-2.89	920.51
Model IIb	16.56	-4.26	35.51	0.5239	5.54	-3.21	926.97
Model IIIb	6.70	-1.56	36.24	0.5501	2.90	-2.34	917.38

We compare the fit of Models Ib and IIIb using the quantile functions in Figures 3 and 4. Both models produced significantly improved fit compared with Figures 1 and 2. The fatigue-limit parameter slightly increased, and the 0.05 quantile converges rapidly to its asymptote as the equivalent stress approaches the fatigue limit. In both cases, the data remain mostly partitioned by the median into the two experiment types.

### 2.3. Model comparison

Using a classical approach, we compute some popular information criteria, such as the Akaike information criterion (AIC) [22], Bayesian information criterion (BIC) [23, 24], and AIC with correction [25], which are based on the maximized log-likelihood values. Such measures consider the goodness of fit and complexity of the models regarding the number of parameters. Table 3 contains the maximum log-likelihood values corresponding to the models introduced in Section 2.2 and the classical information criterion computations.

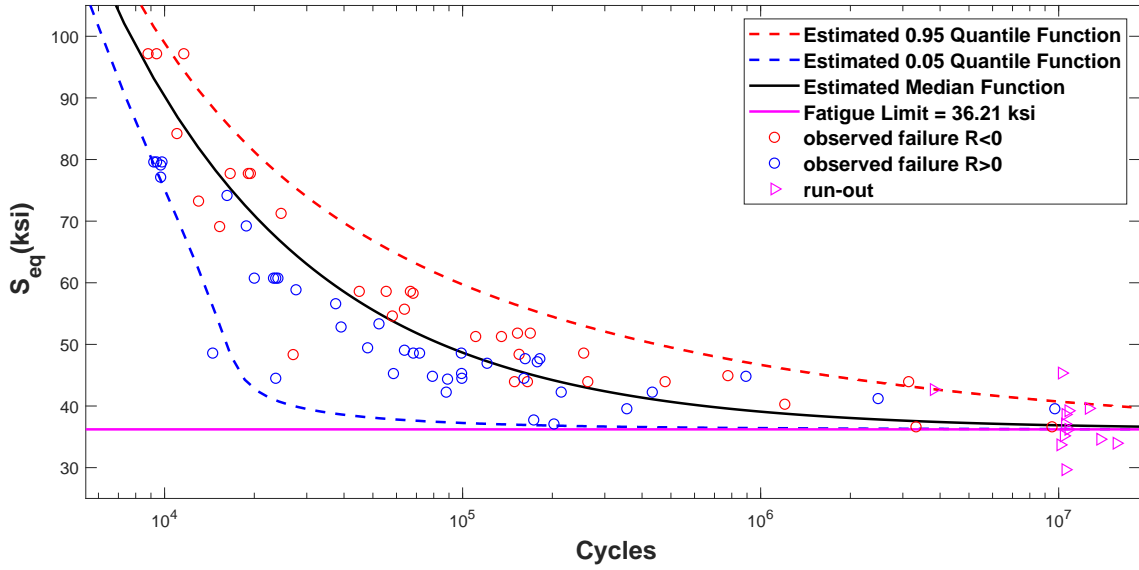


Figure 3: Model Ib:  $\log_{10}(N) \sim N(\mu(S_{eq}), \sigma(S_{eq}))$  and  $S_{eq} = S_{max}(1 - R)^q$ .

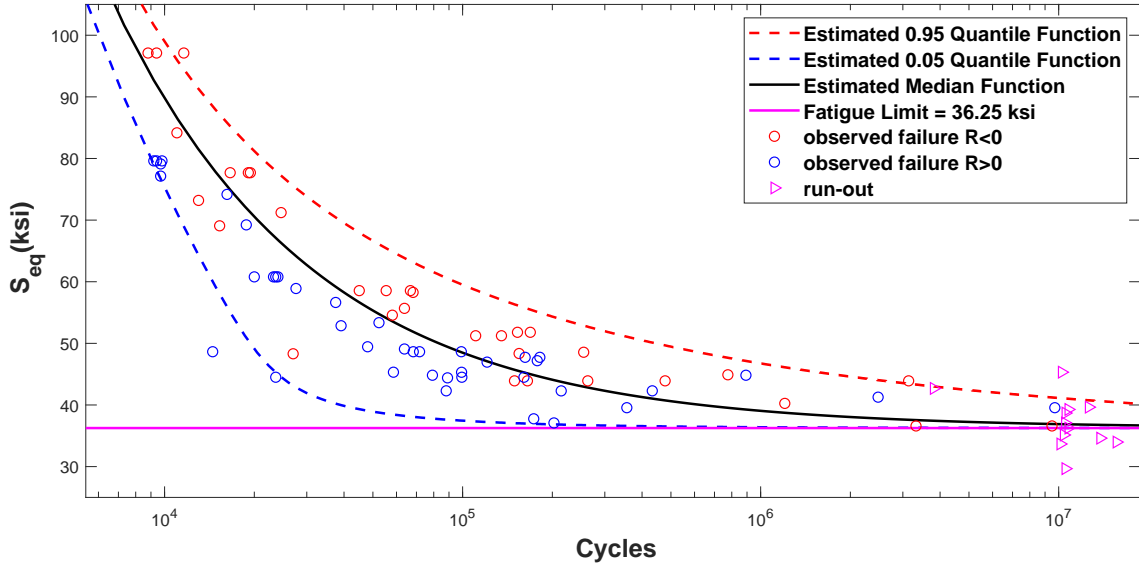


Figure 4: Model IIIb:  $\log_{10}(N) \sim BS(\alpha(S_{eq}), \mu(S_{eq}))$  and  $S_{eq} = S_{max}(1 - R)^q$ .

Table 3: Classical information criteria.

Models	Ia	Ib	IIa	IIb	IIIa	IIIb
Maximum log-likelihood	-950.16	-920.51	-960.68	-926.97	-938.90	-917.38
Akaike information criterion (AIC)	1910.3	1853.0	1931.4	1865.9	1887.8	1846.8
Bayesian information criterion (BIC)	1922.5	1867.7	1943.6	1880.6	1900.0	1861.4
Akaike information criterion with correction	1911.1	1854.1	1932.1	1867.0	1888.5	1847.8

### 3. Analysis of the stress ratio effect and equivalent stress for Dataset 1

In all previous models, the equivalent stress is based on Walker's model [26], which is  $S_{max}(1 - R)^q$ . The following analysis in Table 4 reveals that the parameter  $q$  is related to the sign of the cycle ratio  $R$ .

Table 4: Maximum likelihood estimates for Models I and II with  $S_{eq} = S_{max}(1 - R)^q$ .

Model	Data	$A_1$	$A_2$	$A_3$	$q$	$\tau/\alpha/B_1$	$B_2$	Max log-likelihood
Ia	$R < 0$	7.94	-2.10	61.43	1.37	0.3203	—	-403.56
IIIa	$R < 0$	7.89	-2.10	57.643	1.2753	0.0575	—	-399.64
Ib	$R < 0$	7.44	-1.86	52.56	1.12	5.23	-3.09	-392.86
IIIb	$R < 0$	7.41	-1.85	52.06	1.0986	3.40	-2.50	-392.23
Ia	$R > 0$	6.93	-1.84	34.86	0.6304	0.5561	—	-531.21
IIIa	$R > 0$	6.75	-1.71	35.18	0.6269	0.0974	—	-523.95
Ib	$R > 0$	6.84	-1.75	36.55	0.5410	8.11	-5.07	-500.46
IIIb	$R > 0$	6.75	-1.69	36.62	0.5388	6.27	-4.41	-499.15

Table 5: Maximum likelihood estimates for Models I and II with  $S_{eq} = S_{max}(\frac{1-R}{2})^{1+q}$ .

Model	Data	$A_1$	$A_2$	$A_3$	$q$	$\tau/\alpha/B_1$	$B_2$	Max log-likelihood
Ia	$R < 0$	7.08	-2.11	23.80	0.3679	0.3203	—	-403.56
IIIa	$R < 0$	7.09	-2.10	23.81	0.2754	0.0575	—	-399.64
Ib	$R < 0$	6.82	-1.86	24.26	0.1156	4.19	-3.09	-392.86
IIIb	$R < 0$	6.80	-1.85	24.31	0.0986	2.57	-2.50	-392.23
Ia	$R > 0$	6.59	-1.84	22.52	-0.3696	0.5561	—	-531.21
IIIa	$R > 0$	6.43	-1.71	22.78	-0.3732	0.0974	—	-523.95
Ib	$R > 0$	6.56	-1.75	25.12	-0.4590	7.29	-5.07	-500.46
IIIb	$R > 0$	6.54	-1.74	25.19	-0.4607	5.68	-4.49	-499.13

In Table 4, the fatigue-limit parameter,  $A_3$ , has a different scale based on the stress ratio. We divided  $1 - R$  by 2 in the equivalent stress formula to solve this. However, the estimated values of  $q$  do not change. Therefore, we defined the equivalent stress as  $S_{max}(\frac{1-R}{2})^{1+q}$  or  $S_a(\frac{1-R}{2})^q$ , where  $S_a$  denotes the stress amplitude. Then, we recalibrated the proposed models in Table 5. The fatigue-limit parameter has the same scale for  $R > 0$  and  $R < 0$ . In contrast, the estimated value of  $q$  changes signs with  $R$ . Thus, it seems reasonable to propose the following equivalent stress:

$$S_{eq} = S_{max} \left( \frac{1 - R}{2} \right)^{1 - \text{sign}(R)q} \quad . \quad (3)$$

Next, we calibrate the parameters using the full data ( $R > 0$  and  $R < 0$ ). Table 6 presents the MLEs of Models Ia, IIIa, Ib, and IIIb, along with the maximum log-likelihood and AIC values. The fit is considerably improved in all cases using the equivalent stress 3.

Figures 5 and 6 illustrate the new quantile functions of Models Ia and IIIa with improved equivalent stress 3. The variance is reduced compared to quantiles in Figures 1 and 2. In addition, the two data types are well distributed around the median. Furthermore, the fit can be slightly improved by adapting Huang's model [27] for  $R > 0.5$ .

Table 6: Maximum likelihood estimates for Models I and II with  $S_{eq} = S_{max}(\frac{1-R}{2})^{1-\text{sign}(R)q}$ .

Model	$A_1$	$A_2$	$A_3$	$q$	$\tau/\alpha/B_1$	$B_2$	Max log-likelihood	AIC
Ia	6.99	-2.09	23.72	0.4310	0.4797	—	-942.55	1895.1
IIIa	6.81	-1.95	23.98	0.4336	0.0845	—	-930.85	1871.7
Ib	6.58	-1.76	24.56	0.4433	5.97	-4.23	-899.36	1810.7
IIIb	6.54	-1.74	24.62	0.4436	4.38	-3.65	-897.67	1807.3

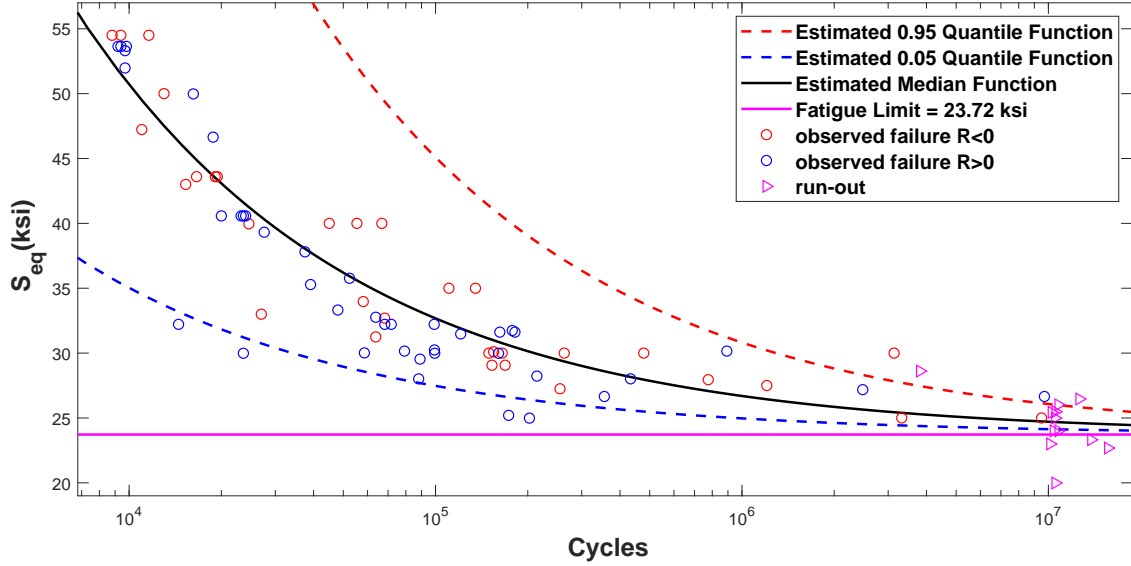


Figure 5: Model Ia:  $\log_{10}(N) \sim N(\mu(S_{eq}), \sigma)$  and  $S_{eq} = S_{max}(\frac{1-R}{2})^{1-\text{sign}(R)q}$ .

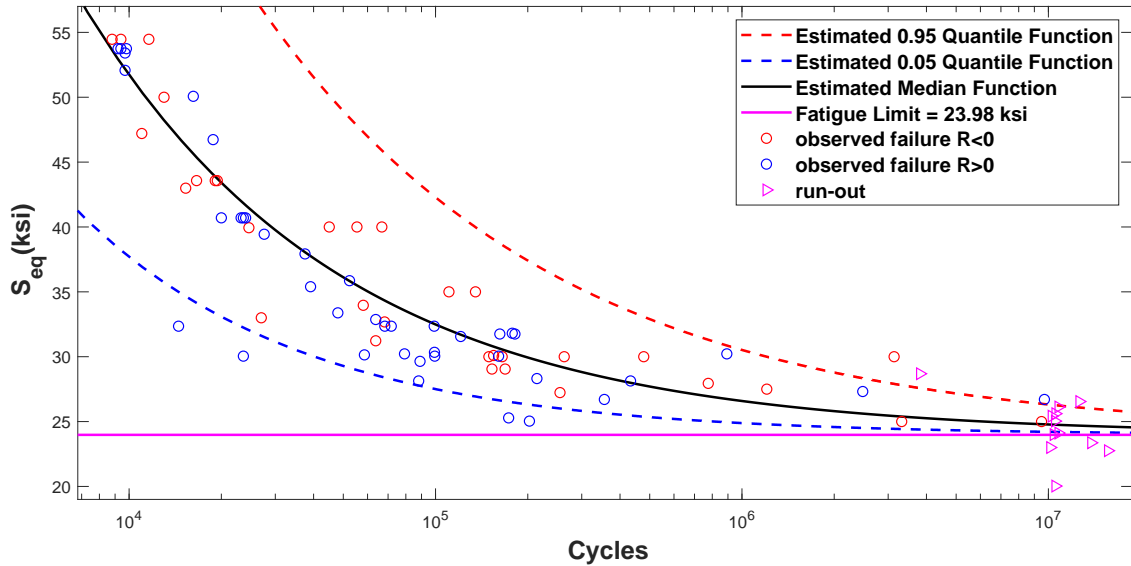


Figure 6: Model IIIa:  $\log_{10}(N) \sim BS(\alpha, \mu(S_{eq}))$  and  $S_{eq} = S_{max}(\frac{1-R}{2})^{1-\text{sign}(R)q}$ .

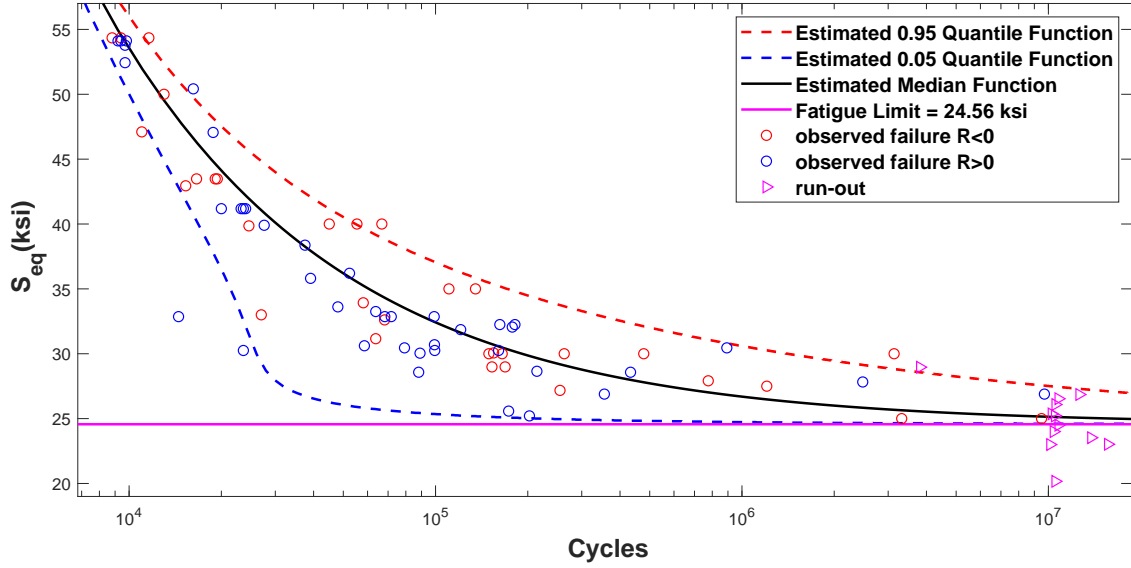


Figure 7: Model Ib:  $\log_{10}(N) \sim N(\mu(S_{eq}), \sigma(S_{eq}))$  and  $S_{eq} = S_{max}(\frac{1-R}{2})^{1-\text{sign}(R)q}$ .

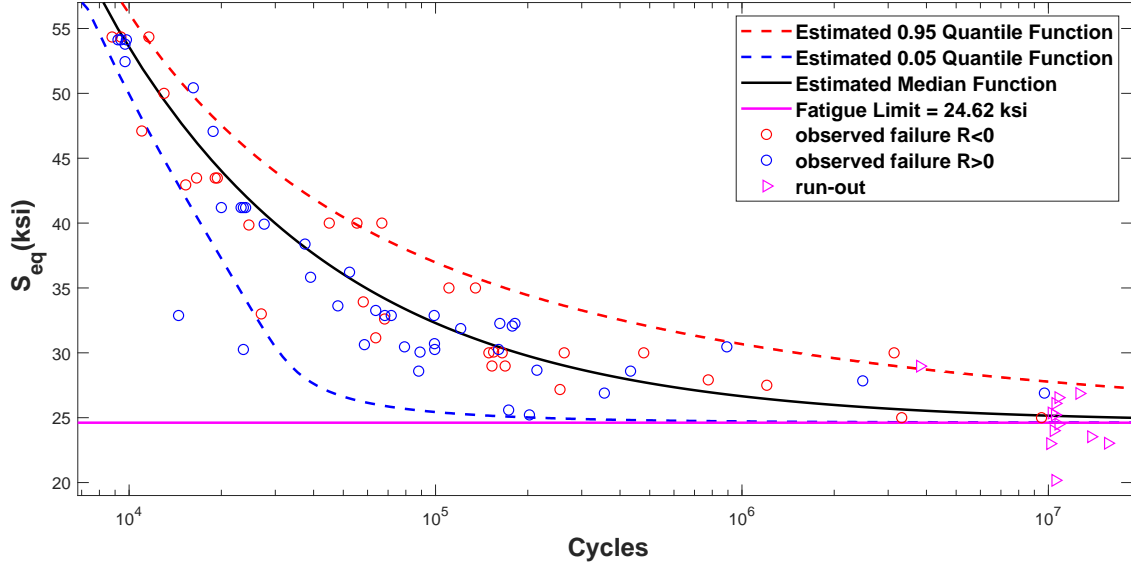


Figure 8: Model IIIb:  $\log_{10}(N) \sim BS(\alpha(S_{eq}), \mu(S_{eq}))$  and  $S_{eq} = S_{max}(\frac{1-R}{2})^{1-\text{sign}(R)q}$ .

### 3.1. Profile likelihood

We compare the profile likelihood of the fatigue limit obtained using the four previous models. Figure 9 depicts the profile likelihood of the fatigue limit,  $A_3$ , using Models Ia and IIIa. For constant variance and shape parameters, the estimated profile likelihood using the Birnbaum–Saunders distribution (Model IIIa) has a noticeably higher mode and a lower variance than Model Ia, which uses the normal distribution. When adopting nonconstant variance and shape parameters, the difference between the two profile likelihoods is negligible, as displayed in Figure 10.

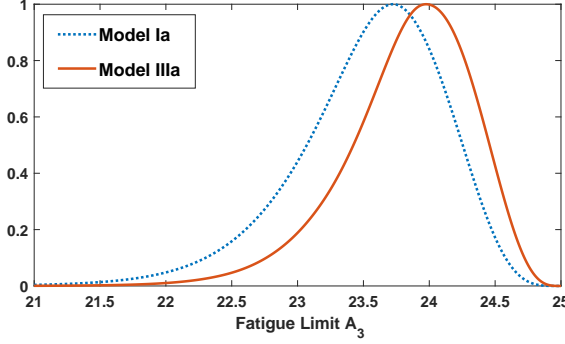


Figure 9: Profile likelihoods of the fatigue-limit parameters using Models Ia and IIIa.

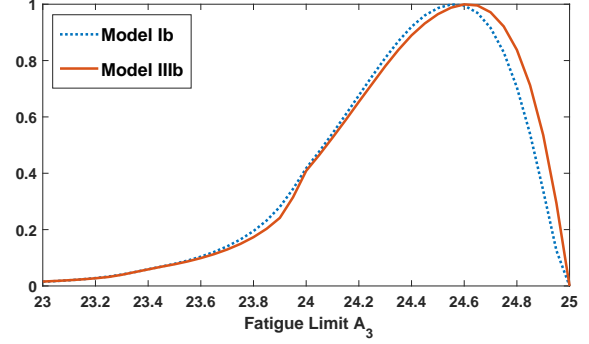


Figure 10: Profile likelihoods of the fatigue-limit parameters using Models Ib and IIIb.

### 3.2. Survival functions

We closely examined the survival functions obtained by calibrated Models Ia, Ib, IIIa, and IIIb at different values of  $S_{max}$  and  $R$  in Figure 11. The Birnbaum–Saunders model (Model IIIa) outperformed the counterpart Gaussian model (Model Ia) because it offers a higher survival probability before the observed failure and a lower survival probability after the observed failure. For Models IIIa and IIIb, the resulting survival probabilities are almost identical for both distributions.

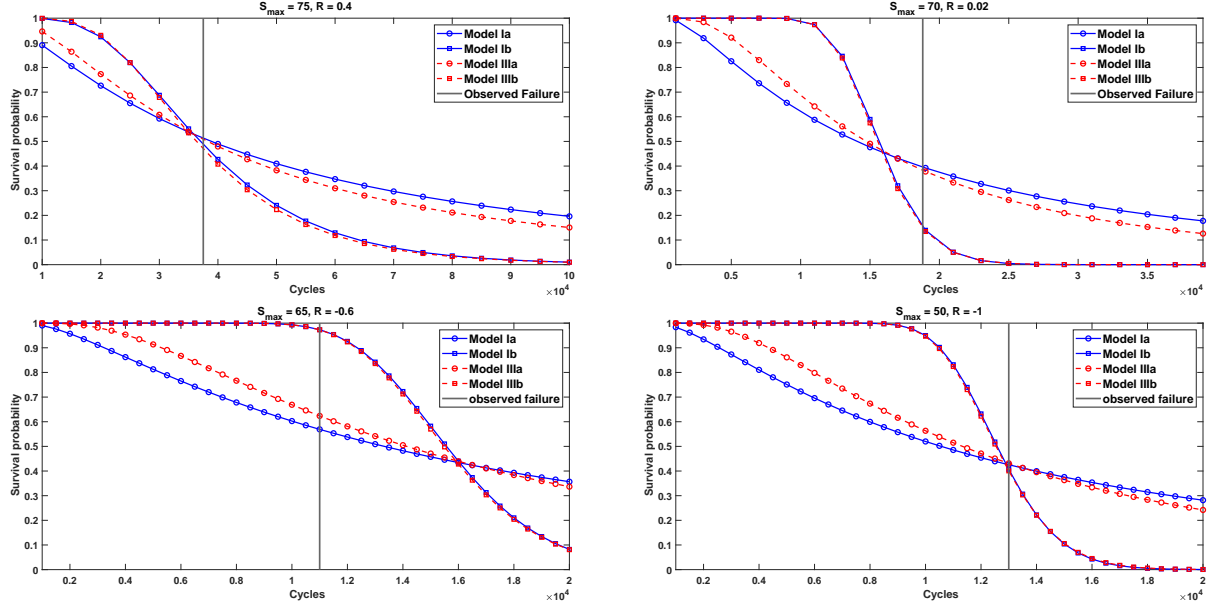


Figure 11: Survival functions of Dataset 1 specimens using calibrated Models Ia, Ib, IIIa, and IIIb for different values of  $S_{max}$  and  $R$ .

## 4. Model calibration and comparison for Dataset 2

### 4.1. Description of Dataset 2

This section introduces and studies new datasets for unnotched specimens of 75S-T6 aluminum alloys [20]. These datasets correspond to 101 round bar specimens with five minimum-section diameters. In

Dataset 2, the fatigue experiments are rotating-bending, and the stress ratio is  $-1$ . Out of the 101 specimens, 13 experiments are run-outs.

Again, we consider fatigue-limit Models Ia, Ib, IIIa, and IIIb with the new equivalent stress (3) to fit the data introduced in 4.1. As mentioned, the stress ratio for rotating-bending experiments is  $-1$ ; therefore, the equivalent stress equals  $S_{max}$ .

Table 7: Maximum likelihood estimates for Models I and III with  $S_{eq} = S_{max}$ .

Model	Specimen	Diameter	$A_1$	$A_2$	$A_3$	$\tau/\alpha/B_1$	$B_2$	Max log-likelihood
Ia	1	1/8	7.20	-1.73	21.17	0.4420	—	-428.28
Ib	1	1/8	7.36	-1.87	21.11	2.38	-1.87	-425.73
IIIa	1	1/8	7.17	-1.72	21.23	0.0721	—	-426.06
IIIb	1	1/8	7.28	-1.82	21.21	0.88	-1.38	-424.62
Ia	2	1/4	8.21	-2.69	21.86	0.4002	—	-343.94
Ib	2	1/4	7.21	-1.86	22.88	8.70	-6.33	-327.49
IIIa	2	1/4	7.96	-2.48	22.16	0.0604	—	-340.75
IIIb	2	1/4	7.20	-1.85	22.91	6.86	-5.62	-326.85
Ia	All	—	9.03	-3.04	18.68	0.5626	—	-1357.8
Ib	All	—	8.23	-2.50	20.49	3.39	-2.53	-1338.1
IIIa	All	—	8.73	-2.84	19.24	0.0880	—	-1349.6
IIIb	All	—	8.15	-2.45	20.61	1.86	-2.02	-1336.1

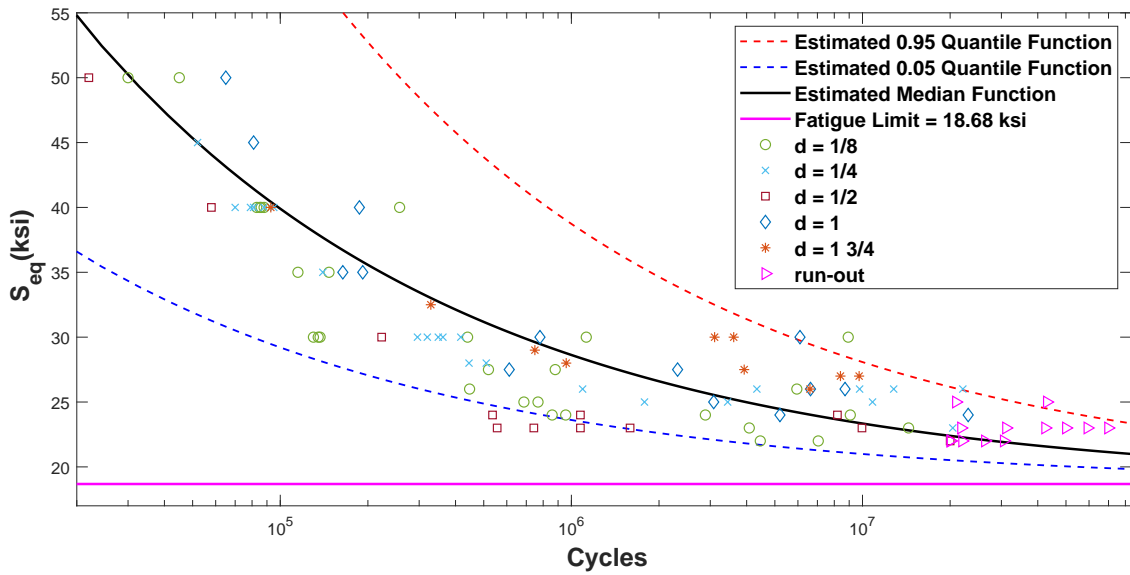


Figure 12: Model Ia:  $\log_{10}(N) \sim N(\mu(S_{eq}), \sigma)$  and  $S_{eq} = S_{max}$ .

Table 7 provides the MLEs for Models Ia, Ib, IIIa, and IIIb when separately fitting Specimen 1 and 2. The joint fit for all specimens is also provided. The goodness of fit and estimated fatigue limit decreased when the data were combined. Figures 12 and 13 reveal the quantiles of calibrated Models Ia and Ib, respectively.

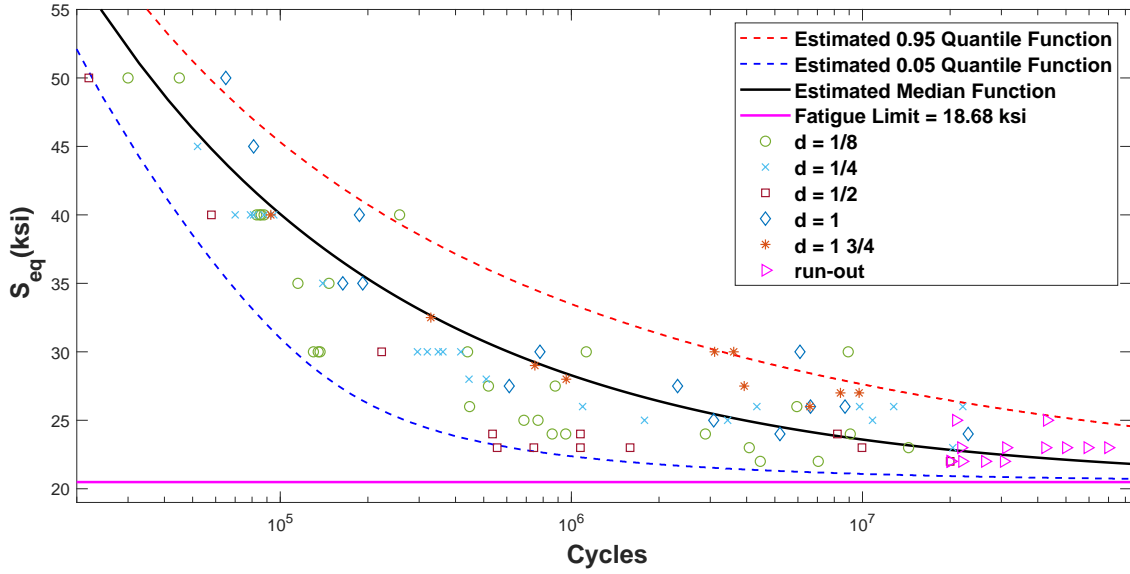


Figure 13: Model Ib:  $\log_{10}(N) \sim N(\alpha(S_{eq}), \mu(S_{eq}))$  and  $S_{eq} = S_{max}$ .

#### 4.2. Profile likelihood and confidence intervals

We again compared the profile likelihood of the fatigue limit obtained using the four previous models using Dataset 2 instead. Figure 14 displays the profile likelihood of the fatigue limit,  $A_3$ , using Models Ia and IIIa. As concluded, the profile likelihood when using the Birnbaum–Saunders distribution (Model IIIa) has a higher mode and much lower variance than Model Ia. With nonconstant variance and shape parameters, the two profile likelihoods are almost identical 10.

We confirmed the mentioned conclusions by estimating the confidence intervals of the pooled MLEs, given that Dataset 2 is complete. The confidence intervals presented in Table 8 are obtained by stratified bootstrapping where the sampled dataset maintains the same proportions in the original data related to the five specimens. The results indicate that the Birnbaum–Saunders distribution provides tighter confidence intervals than the normal distribution, especially when using a constant variance. This property is essential to generate accurate survival and failure predictions.

Table 8: Confidence intervals of 90% for the pooled maximum likelihood estimates for Models I and III.

Model	$A_1$	$A_2$	$A_3$	$\tau/\alpha/B_1$	$B_2$
Ia	(7.9, 11.1)	(-4.3, -2.2)	(14.3, 21)	(0.49, 0.62)	—
Ib	(7.6, 9.2)	(-3.1, -2.1)	(18.5, 21.6)	(2.8, 4.6)	(-3.4, -2.1)
IIa	(7.8, 10.3)	(-3.8, -2.2)	(15.7, 21.1)	(0.077, 0.096)	—
IIb	(7.6, 9.1)	(-3.1, -2.0)	(18.6, 21.7)	(1.3, 3)	(-2.9, -1.6)

#### 4.3. Survival functions

Figure 16 depicts the survival probabilities of specimens from Dataset 2 under different settings using calibrated models by the pooled or specific specimen data.

Comparing the results for Datasets 1 and 2, we notice higher variability in the latter, especially when using pooled Dataset 2 with multiple specimens of different geometries and sizes. The fit results could

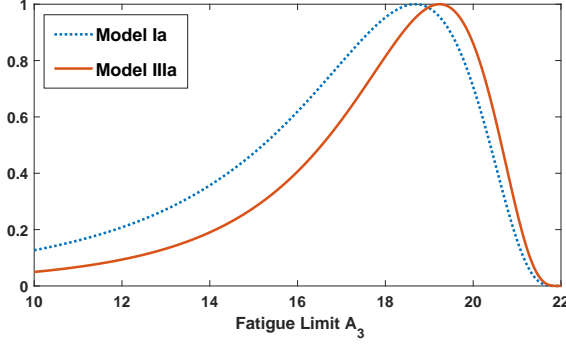


Figure 14: Profile likelihoods of the fatigue-limit parameters using Models Ia and IIIa.

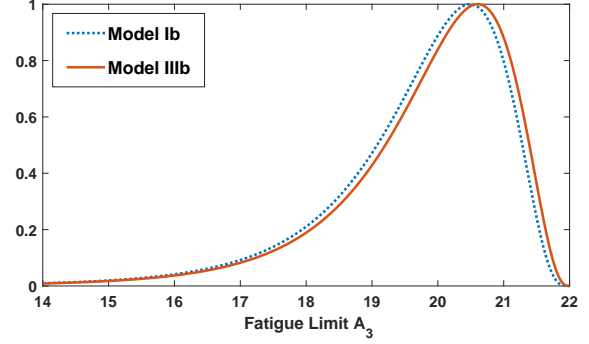


Figure 15: Profile likelihoods of the fatigue-limit parameters using Models Ib and IIIb.

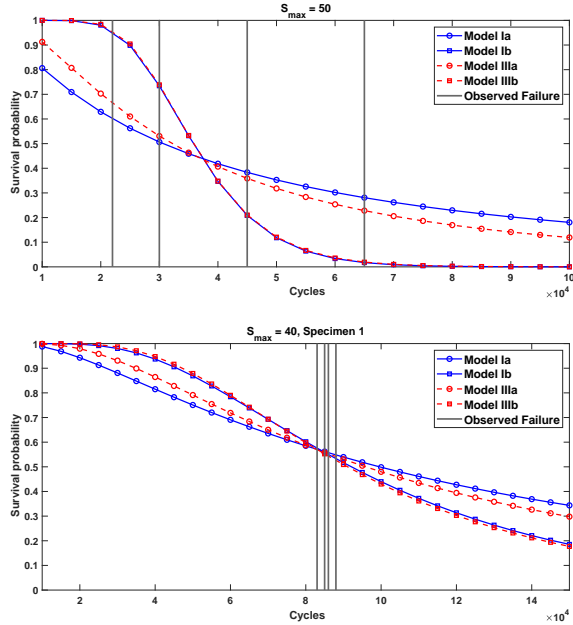


Figure 16: Survival functions of Dataset 2 specimens using calibrated Models Ia, Ib, IIIa, and IIIb for values of  $S_{max}$  and  $R$ .

be improved using Poisson models that consider the geometry and size of the specimen [28]. However, implementing and analyzing such models is beyond the scope of the current work.

## 5. Model calibration and comparison for Dataset 3

### 5.1. Description of Dataset 3

To generalize the previous results, we consider a well-known dataset: the laminate panel S-N dataset [21, 5]. This dataset contains fatigue data for 125 carbon eight-harness-satin/epoxy laminate specimens subjected to four-point out-of-plane bending tests, where 10 out of 125 experiments are run-outs. In this case, the equivalent stress needed in the fatigue-limit models is given directly in the data, and we do not have the stress ratio.

As a first illustration, we used probability plots, as suggested in [29]. Figures ?? and ? present the probability plot of the normal distribution and Birnbaum–Saunders distribution as models for the fatigue

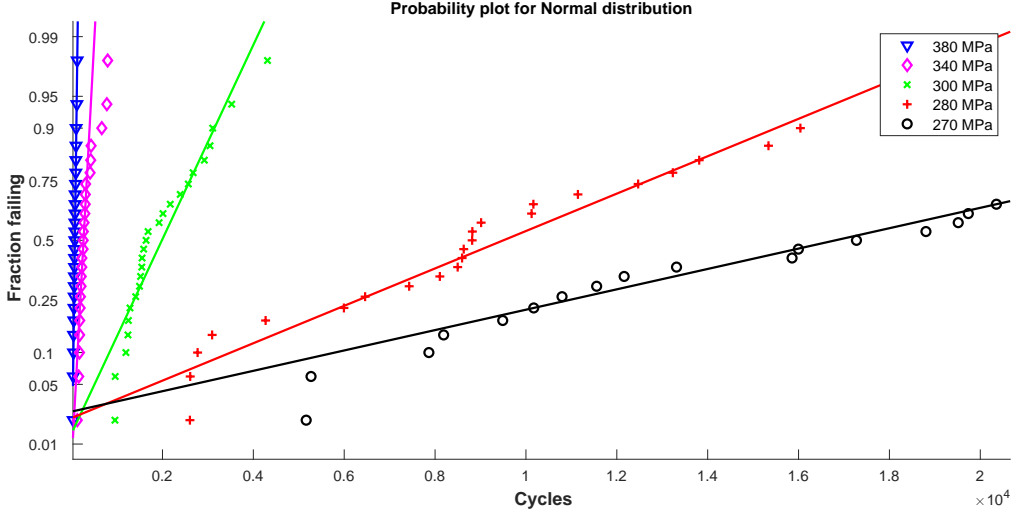


Figure 17: Probability plot of the normal distribution as a model for the number of cycles  $N$ .

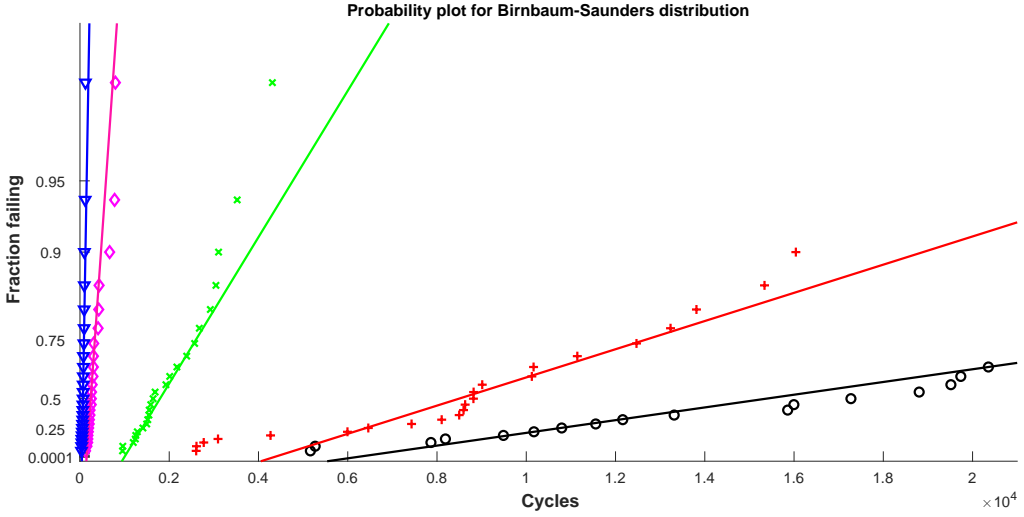


Figure 18: Probability plot of the Birnbaum-Saunders distribution as a model for the number of cycles  $N$ .

life,  $N$ . Modeling  $N$  using the normal or Birnbaum-Saunders distribution is not a good choice. Instead, modeling  $\log(N)$  using these distributions provides better probability plots, as illustrated in Figures ??.

We calibrated six fatigue-limit models: Ia, Ib, IIa, IIb, IIIa, and IIIb, slightly modified using natural instead of base 10 logarithms. This approach was conducted to make the MLE parameters comparable to the results in the literature and does not affect the goodness of fit. We also fit the data using the Weibull distribution but did not include these results, as this distribution consistently provides the worst fit.

Table 9 provides the MLEs for Models Ia, Ib, IIa, IIb, IIIa, and IIIb. Table 10 compares all six models employing classical information criteria. Figures 21 and 22 present the quantiles of calibrated Models Ia and IIIa, respectively. Figures 23 and 24 display the quantiles of calibrated Models Ib and IIIb, respectively.

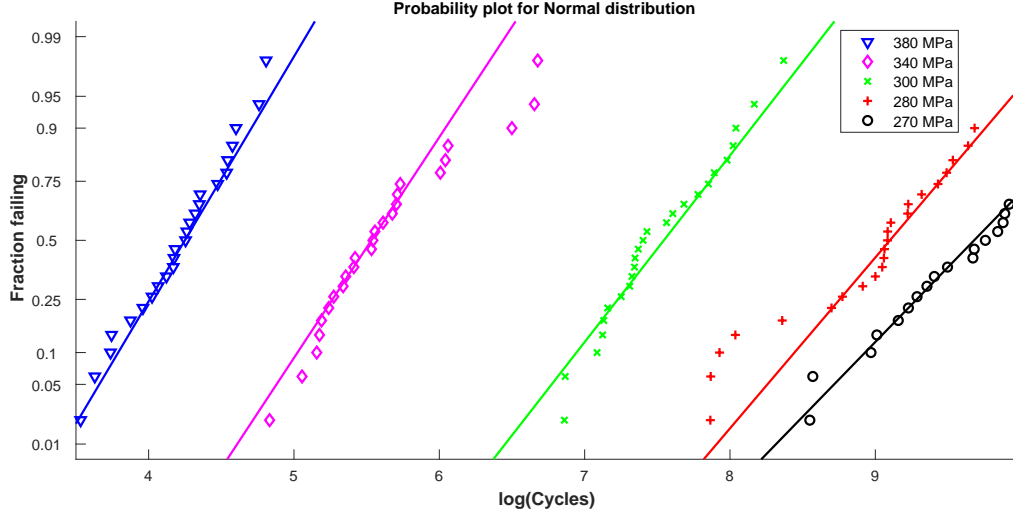


Figure 19: Probability plot of the normal distribution as a model for  $\log(N)$ .

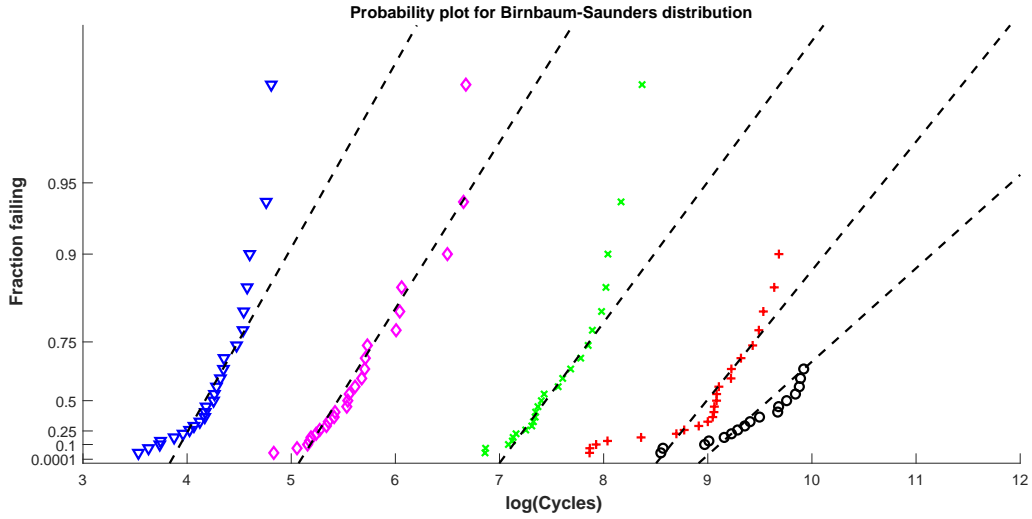


Figure 20: Probability plot of the Birnbaum-Saunders distribution as a model for  $\log(N)$ .

Table 9: Maximum likelihood estimates for Models I, II, and III.

Model	$A_1$	$A_2$	$A_3$	$\tau/\alpha/B_1$	$B_2$	Max log-likelihood
Ia	31.56	-5.32	209.69	0.4902	—	-889.77
Ib	30.26	-5.10	214.22	8.71	-1.64	-885.28
IIa	32.15	-5.43	207.55	0.5031	—	-889.90
IIb	30.77	-5.18	212.45	9.01	-1.69	-885.17
IIIa	29.63	-4.99	216.48	0.0718	—	-885.64
IIIb	30.14	-5.08	214.59	-6.84	0.73	-884.67

Table 10: Classical information criteria.

Models	Ia	Ib	IIa	IIb	IIIa	IIIb
Maximum log-likelihood	-889.77	-885.28	-889.90	-885.17	-885.64	-884.67
Akaike information criterion (AIC)	1787.5	1780.6	1787.8	1780.3	1779.3	1779.3
Bayesian information criterion (BIC)	1798.9	1794.7	1799.1	1794.5	1790.6	1793.5
Akaike information criterion with correction	1787.9	1781.1	1788.1	1780.8	1779.6	1779.8

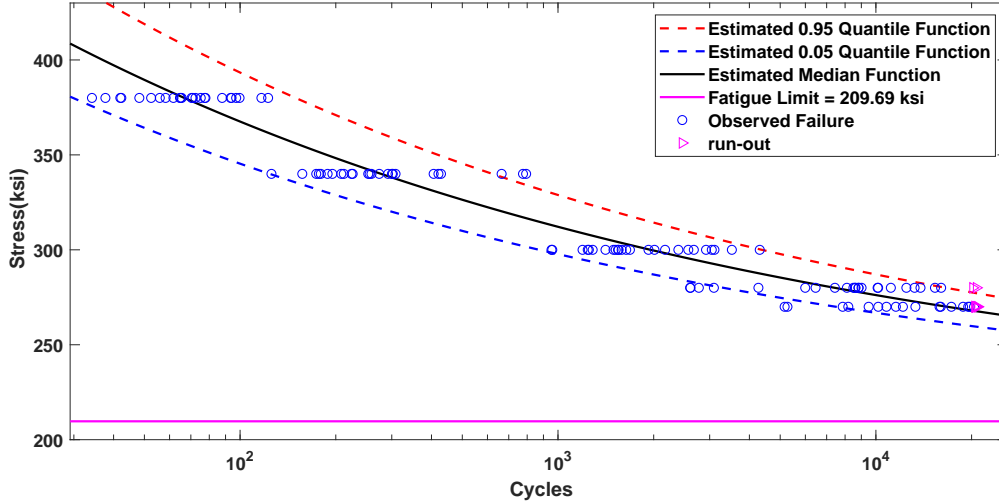


Figure 21: Model Ia:  $\log(N) \sim N(\mu(S), \sigma)$ .

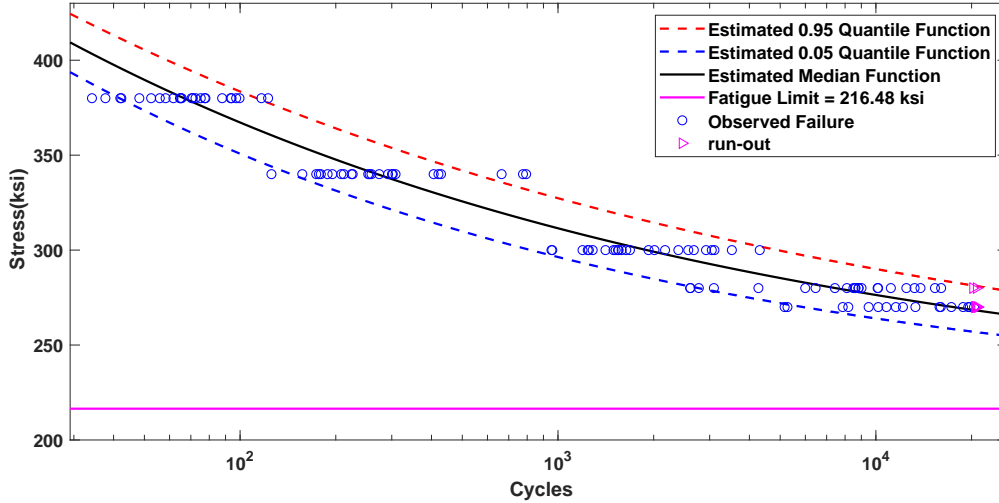


Figure 22: Model IIIa:  $\log(N) \sim BS(\alpha, \mu(S))$ .

## 6. Conclusions

Multiple variants of the fatigue-limit models were calibrated and ranked employing ML and classical information criteria. The proposed approach of modeling the logarithm of the fatigue life using the

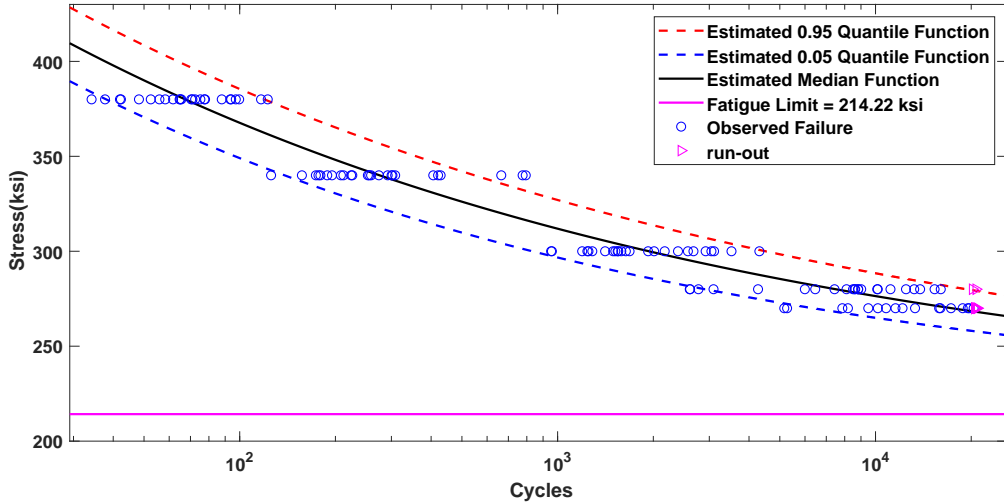


Figure 23: Model Ib:  $\log(N) \sim N(\mu(S), \sigma(S))$ .

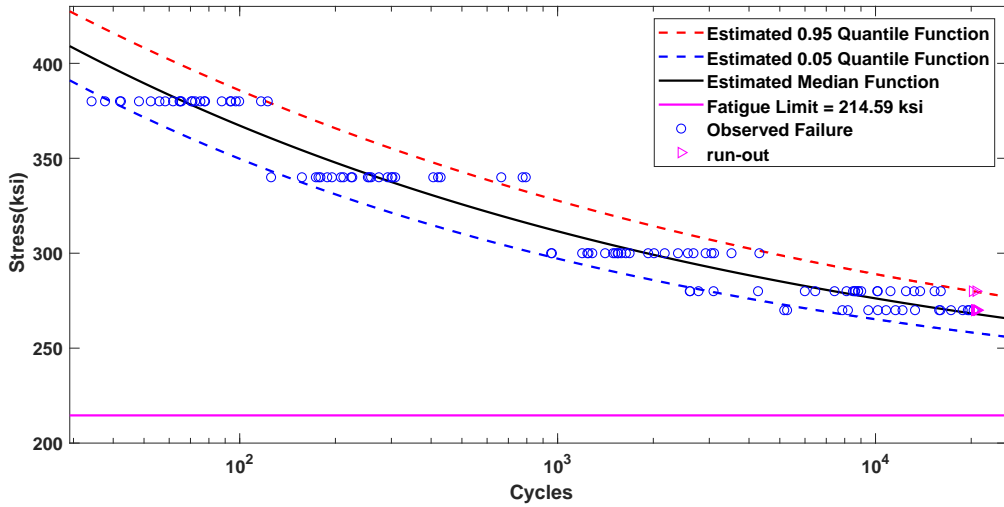


Figure 24: Model IIIb:  $\log(N) \sim BS(\alpha(S), \mu(S))$ .

Birnbaum–Saunders distribution proved to be superior or equivalent to the best model in all cases.

For Dataset 1, fatigue experiments included two types of loadings. We introduced a new equivalent stress to generalize the models for such scenarios. Therefore, the fit for Dataset 1 considerably improved for all models. The suggested equivalent stress does not require adding new parameters and could be used for fatigue data with only one loading type.

In Dataset 2, four round bar specimens were subjected to rotating-bending fatigue experiments. The calibration was performed using Specimens 1 and 2 individually. Then, pooled calibration was performed using the full dataset. The variability of the latter calibration increased, which was further analyzed by obtaining confidence intervals of the MLEs via bootstrapping.

Laminate panel data were adopted in Section 5. Models I, II, and III were calibrated and ranked using constant and nonconstant variance/shape parameters. The fit results confirmed that Birnbaum–Saunders models are better than log-normal and Weibull models, especially when the variance is constant. Model IIIa

is preferable over IIIb when comparing the classical information criteria.

For all calibrated models, we analyzed the data with the estimated S-N curves and survival probabilities in the three datasets. The various models were compared using AIC, BIC, and AIC with correction. Profile likelihoods were also computed for the fatigue-limit parameter.

The Birnbaum–Saunders distribution provided a better fit for data and higher confidence in estimating the fatigue-limit parameter in Model IIIa. Models Ib and IIIb yielded similar results regarding information criteria, survival probabilities, and profile likelihood. A nonconstant variance with the log-normal distribution could be an alternative to the proposed Birnbaum–Saunders model in some frameworks.

## References

- [1] J. Schijve, Fatigue of structures and materials in the 20th century and the state of the art, *International Journal of Fatigue* 25 (8) (2003) 679–702.
- [2] J. Schijve, *Fatigue of Structures and Materials*, 2nd Edition, Springer, 2009.
- [3] A. Fatemi, L. Yang, Cumulative fatigue damage and life prediction theories: a survey of the state of the art for homogeneous materials, *International Journal of Fatigue* 20 (1) (1998) 9–34.
- [4] I. Babuska, Z. Sawlan, M. Scavino, B. Szabó, R. Tempone, Bayesian inference and model comparison for metallic fatigue data, *Computer Methods in Applied Mechanics and Engineering* 304 (2016) 171–196.
- [5] F. G. Pascual, W. Q. Meeker, Analysis of fatigue data with runouts based on a model with nonconstant standard deviation and a fatigue limit parameter, *Journal of Testing and Evaluation* 25 (1997) 292–301.
- [6] F. G. Pascual, W. Q. Meeker, Estimating fatigue curves with the random fatigue-limit model, *Technometrics* 41 (4) (1999) 277–289.
- [7] K. J. Ryan, Estimating expected information gains for experimental designs with application to the random fatigue-limit model, *Journal of Computational and Graphical Statistics* 12 (3) (2003) 585–603.
- [8] J. Schijve, A normal distribution or a Weibull distribution for fatigue lives, *Fatigue & Fracture of Engineering Materials & Structures* 16 (8) (1993) 851–859.
- [9] Z. Birnbaum, S. Saunders, A new family of life distributions, *Journal of Applied Probability* 6 (2) (1969) 319–327. [doi:10.2307/3212003](https://doi.org/10.2307/3212003).
- [10] Z. W. Birnbaum, S. C. Saunders, Estimation for a family of life distributions with applications to fatigue, *Journal of applied probability* 6 (2) (1969) 328–347.
- [11] M. Engelhardt, L. J. Bain, F. T. Wright, Inferences on the parameters of the Birnbaum–Saunders fatigue life distribution based on maximum likelihood estimation, *Technometrics* 23 (3) (1981) 251–256. [doi:10.1080/00401706.1981.10486294](https://doi.org/10.1080/00401706.1981.10486294).
- [12] J. A. Achcar, Inferences for the Birnbaum–Saunders fatigue life model using Bayesian methods, *Computational statistics & data analysis* 15 (4) (1993) 367–380.
- [13] E. G. Tsionas, Bayesian inference in Birnbaum–Saunders regression, *Communications in Statistics- Theory and Methods* 30 (1) (2001) 179–193.

- [14] A. Xu, Y. Tang, Bayesian analysis of Birnbaum–Saunders distribution with partial information, *Computational Statistics & Data Analysis* 55 (7) (2011) 2324–2333.
- [15] J. R. Rieck, J. R. Nedelman, A log-linear model for the Birnbaum–Saunders distribution, *Technometrics* 33 (1) (1991) 51–60.
- [16] D. Kundu, Bivariate log Birnbaum–Saunders distribution, *Statistics* 49 (4) (2015) 900–917.
- [17] V. Leiva, *The Birnbaum–Saunders Distribution*, Academic Press, 2015.
- [18] N. Balakrishnan, D. Kundu, Birnbaum–Saunders distribution: A review of models, analysis, and applications, *Applied Stochastic Models in Business and Industry* 35 (1) (2019) 4–49.
- [19] H. J. Grover, S. M. Bishop, L. R. Jackson, Fatigue Strengths of Aircraft Materials. Axial-Load Fatigue Tests on Unnotched Sheet Specimens of 24S-T3 and 75S-T6 Aluminum Alloys and of SAE 4130 Steel NACA TN 2324, National Advisory Committee on Aeronautics (March 1951).
- [20] W. S. Hyler, R. A. Lewis, H. J. Grover, Experimental Investigation of Notch-Size Effects on Rotating-Beam Fatigue Behavior of 75S-T6 Aluminum Alloys NACA TN 3291, National Advisory Committee on Aeronautics (November 1954).
- [21] T. Shimokawa, Y. Hamaguchi, Statistical evaluation of fatigue life and fatigue strength in circular-hole notched specimens of a carbon eight-harness-satin/epoxy laminate, *Statistical research on fatigue and fracture(A 88-51351 22-39)*. London and New York, Elsevier Applied Science, 1987, (1987) 159–176.
- [22] H. Akaike, Information theory and an extension of the maximum likelihood principle, in: *Breakthroughs in Statistics*, Volume I, Springer, 1992, pp. 610–624.
- [23] G. Schwarz, et al., Estimating the dimension of a model, *Ann. Statist.* 6 (2) (1978) 461–464.
- [24] A. A. Neath, J. E. Cavanaugh, The Bayesian information criterion: background, derivation, and applications, *Wiley Interdisciplinary Reviews: Computational Statistics* 4 (2) (2012) 199–203.
- [25] K. P. Burnham, D. R. Anderson, *Model Selection and Multimodel Inference*, 2nd Edition, Springer, 2002.
- [26] K. Walker, The effect of stress ratio during crack propagation and fatigue for 2024-t3 and 7075-t6 aluminum, *Effects of environment and complex load history on fatigue life* 462 (1970) 1–14.
- [27] X. Huang, T. Moan, Improved modeling of the effect of R-ratio on crack growth rate, *International Journal of fatigue* 29 (4) (2007) 591–602.
- [28] I. Babuška, Z. Sawlan, M. Scavino, B. Szabó, R. Tempone, Spatial poisson processes for fatigue crack initiation, *Computer Methods in Applied Mechanics and Engineering* 345 (2019) 454–475.
- [29] W. Q. Meeker, L. A. Escobar, F. G. Pascual, Y. Hong, P. Liu, W. M. Falk, B. Ananthasayanam, Modern statistical models and methods for estimating fatigue-life and fatigue-strength distributions from experimental data, *arXiv preprint arXiv:2212.04550*.